Inorganic Chemistry

ARTICLE

pubs.acs.org/IC

Polyoxomolybdate Promoted Hydrolysis of a DNA-Model Phosphoester Studied by NMR and EXAFS Spectroscopy

Gregory Absillis,[†] Rik Van Deun,[‡] and Tatjana N. Parac-Vogt*[,†]

[†]Department of Chemistry, Katholieke Universiteit Leuven, Celestijnenlaan 200F, B-3001 Leuven, Belgium

[‡]Inorganic and Physical Chemistry Department, Universiteit Gent, Krijgslaan 281, Building S3, B-9000 Gent, Belgium

ABSTRACT:

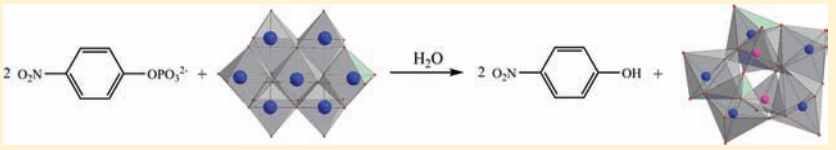

Hydrolysis of (*p*-nitrophenyl)phosphate (NPP), a commonly used phosphatase model substrate, was examined in molybdate solutions by means of ^{1}H, ^{31}P, and ^{95}Mo NMR spectroscopy and Mo K-edge Extended X-ray Absorption Fine Structure (EXAFS) spectroscopy. At 50 °C and pD 5.1 the cleavage of the phosphoester bond in NPP proceeds with a rate constant of 2.73×10^{-5} s^{-1} representing an acceleration of nearly 3 orders of magnitude as compared to the hydrolysis measured in the absence of molybdate. The pD dependence of k_{obs} exhibits a bell-shaped profile, with the fastest cleavage observed in solutions where $[Mo_7O_{24}]^{6-}$ is the major species in solution. Mixing of NPP and $[Mo_7O_{24}]^{6-}$ resulted in formation of these two intermediate complexes that were detected by ^{31}P NMR spectroscopy. Complex A was characterized by a ^{31}P NMR resonance at −4.27 ppm and complex B was characterized by a ^{31}P NMR resonance at −7.42 ppm. On the basis of the previous results from diffusion ordered NMR spectroscopy, performed with the hydrolytically inactive substrate phenylphosphonate (PhP), the structure of these two complexes was deduced to be $(NPP)_2Mo_5O_{21}^{4-}$ (complex A) and $(NPP)_2Mo_{12}O_{36}(H_2O)_6^{4-}$ (complex B). The pH studies point out that both complexes are hydrolytically active and lead to the hydrolysis of phosphoester bond in NPP. The NMR spectra did not show evidence of any paramagnetic species, excluding the possibility of Mo(VI) reduction to Mo(V), and indicating that the cleavage of the phosphomonoester bond is purely hydrolytic. The Mo K-edge XANES region also did not show any sign of Mo(VI) to Mo(V) reduction during the hydrolytic reaction. ^{95}Mo NMR and Mo K-edge EXAFS spectra measured during different stages of the hydrolytic reaction showed a gradual disappearance of $[Mo_7O_{24}]^{6-}$ during the hydrolytic reaction and appearance of $[P_2Mo_5O_{23}]^{6-}$, which was the final complex observed at the end of hydrolytic reaction.

INTRODUCTION

Early transition metals such as V, Nb, Ta, Mo, and W in their highest oxidation state are able to form negatively charged metal-oxide clusters, commonly known as polyoxometalates (POMs). This class of compounds is characterized by a broad variety of chemical and physical properties and exhibits a wide structural versatility. Accordingly, many applications in various research domains, including medicine and catalysis have been reported.[1−4] It has been demonstrated that because of their strong acidity and tunable redox properties, several heteropolyacids were used both in homogeneous and heterogeneous catalysis.[5−9] In the past decade there has been a growing interest in the biological activity of POMs, especially after it was shown that many of them have potent antiviral, antibacterial, and antitumor properties.[10−15] It has been generally accepted that noncovalent binding influenced by the size, shape, and charge density of polyoxometalates is the main factor governing their biological activity, but on the other hand, very little is known about the reactivity of POMs towards biological molecules and their building blocks.

Among the POMs exhibiting biological activity, the polyoxomolybdate $[Mo_7O_{24}]^{6-}$ has been extensively studied. A number of in vivo studies have shown that it exhibits antitumor properties against a range of different cancer cell lines, including the highly recalcitrant pancreatic cancer cells, and that its activity is comparable to that of commercially available drugs.[16−21] Despite the fact that the antitumor activity of polyoxomolybdate has been well documented, its mode of action on a molecular level has not been fully understood. Several studies have shown that polyoxomolybdates interact with biological molecules containing phosphate moieties, leading to the formation of a pentamolybdodiphosphate type of structure.[22−26] In the presence of molybdate, the high energy phospoanhydride bonds in ATP are fully hydrolyzed.[27−29] Several studies implicate the interaction of molybdate with phosphate groups in ATP as one of the key factors in the antitumor activity of $[Mo_7O_{24}]^{6-}$.[26−29]

Interestingly, although there is much literature data on the interactions between polyoxomolybdates and phosphate moieties, the interactions with monophosphoesters have been scarcely explored. The hydrolysis of monophosphates is commonly described as one of the most important reactions in biological systems. Monophosphates are involved in several essential processes such as signal transduction, energy storage, and replication of genetic material.[30] While most nucleases utilize metal ions

Received: July 14, 2011
Published: October 26, 2011

dx.doi.org/10.1021/ic201498u | *Inorg. Chem.* 2011, 50, 11552–11560

as cofactors, the exact role of the metal in the hydrolytic mechanism is not fully understood. Numerous model compounds have been used to identify the possible mechanism by which metal ions promote phosphoester bond hydrolysis.[31−35] With the exception of the work by Yatsimirsky and his co-workers, in which charge neutral lanthanide complexes have been implicated as hydrolytically active species,[36] the metal complexes that are active as catalysts for the hydrolysis of phosphoester bonds are generally positively charged.[37−42] This seems to be an essential property for electrostatic interaction with the negatively charged phosphate group. The mechanism by which metal complexes accelerate the rate of phosphate ester hydrolysis is generally described as an interplay of several factors among which the Lewis acid activation via coordination of phosphoryl oxygen(s) to the metal ion, coordination of a nucleophile such as water or hydroxide ligand to the metal, and leaving group activation via coordination of the leaving group oxygen to the metal appear to be of crucial importance.[30−33] As a result, the metal complexes that act as artificial phosphoesterases have to meet a number of criteria such as an overall positive charge, free coordination site for the binding of the phosphoryl oxygen, the presence of coordinated water or hydroxide, or the presence of functional groups for acid−base catalysis, among others.

Despite these requirements, our recent studies have revealed that $[Mo_7O_{24}]^{6-}$, which is a negatively charged and coordinatively saturated metal complex, lacking coordinated water or hydroxide, effectively hydrolyses phosphodiester bonds in bis-(*p*-nitrophenyl) phosphate (BNPP) and 2-hydroxypropyl-4-nitrophenyl phosphate (HPNP), commonly used as DNA and RNA model compounds.[43,44] These kinetic studies strongly suggest that $[Mo_7O_{24}]^{6-}$ is the hydrolytically active complex and that the cleavage occurs by a mechanism which is different to that of other currently known hydrolytically active metal complexes. The evidence suggested that the origin of hydrolytic activity of $[Mo_7O_{24}]^{6-}$ toward phosphodiesters may lay in its high internal lability and an intramolecular exchange process which results in partial detachment of one MoO_4 tetrahedron.[43,44] Because of the rapid exchange between the free and the bound phosphodiester, the structure of the active complex could not be elucidated by spectroscopic techniques. Further to this, the interaction between polyoxomolybdates and (*p*-nitrophenyl)-phosphate (NPP), a commonly used phosphatase model substrate, has been investigated by using the analogous, but hydrolytically inactive model substrate phenylphosphonate (PhP). Two distinct complexes $[(PhP)_2Mo_5O_{21}]^{4-}$ and $[(PhP)Mo_7O_{25}]^{4-}$ could be detected by diffusion ordered NMR spectroscopy (DOSY NMR).[43] On the basis of the DOSY NMR results with PhP, the complexes $(NPP)_2Mo_5O_{21}{}^{4-}$ (complex A) and $(NPP)_2Mo_{12}O_{36}(H_2O)_6{}^{4-}$ (complex B) have been suggested as the active species leading to hydrolysis of the phosphoester bond in the NPP substrate. In this study we further employ kinetics experiments, multinuclear NMR, and Extended X-ray Absorption Fine Structure (EXAFS) spectroscopy to fully examine the hydrolysis of NPP in the presence of polyoxomolybdates and give a complete account on this novel reaction.

EXPERIMENTAL SECTION

Materials. Sodium molybdate, (*p*-nitrophenyl)phosphate, and phenylphosphate were purchased from Acros and used without further purification. The pH of the solutions for the NMR studies was adjusted with D_2SO_4 and NaOD, both from Acros.

NMR Spectroscopy. ^1H and ^{31}P spectra were recorded on a Bruker Avance 300 spectrometer and on a Bruker Avance 400 spectrometer. D_2O with 0.05 wt % 3-(trimethylsilyl) propionic acid as an internal standard was used as a solvent. Trimethyl phosphate was used as a 0 ppm ^{31}P reference. ^{95}Mo NMR spectra were recorded on a Bruker Avance 600 (39 MHz) spectrometer. UV−Vis absorption spectra have been measured on a Varian Cary 5000 spectrophotometer.

EXAFS Spectroscopy. Measurements were performed in transmission mode using a Si(111) double crystal monochromator on the Dutch-Belgian Beamline (DUBBLE, BM26A) at the European Synchrotron Radiation Facility (ESRF, Grenoble, France).[46a] Higher harmonics were rejected by the Si mirrors themselves (suppression factor about 1000). The molybdenum K-edge spectra were collected using Oxford Instruments ionization chambers, filled with 30% Ar/70% He at 1 bar for I_0 and pure Ar at 1.5 bar for I_t at ambient temperature and pressure. Data were collected in equidistant *k*-steps of 0.05 $Å^{-1}$ across the EXAFS region. A Mo metal foil (first inflection point at 19999 eV) was used for energy calibration. As the Mo phase function is strongly nonlinear at *k*-values below $k = 5$ $Å^{-1}$, in a first approach, the filtering and back-transformation procedure was made by using only *k*-values larger than $k = 5$ $Å^{-1}$ (*k*-range was then 5−16.9 $Å^{-1}$), but this had only a minor effect on the structural parameters obtained. Therefore, it was decided to use the whole *k*-range from 2.6 to 16.9 $Å^{-1}$ in the final procedure. Solutions of the polyoxomolybdates were pipetted out of the reaction vessel at the indicated times. This vessel was kept at 50 °C, and the solutions were then left to cool to room temperature (thereby slowing down the reaction to a near standstill) and were sealed in polyethylene cuvets with a path length of 8 mm for the EXAFS measurements. The initial $[MoO_4]^{2-}$ concentration had been set to 700 mM and the concentration of NPP was 100 mM. EXAFS data extraction and data fitting were performed using the program EXAFSPAK.[46b] Theoretical phase and amplitude functions were calculated using FEFF 8.2 using the crystal structure from reference 58.[47] The amplitude reduction factor, $S_0{}^2$, was kept constant at 1 throughout the fit.

Kinetics. In a typical kinetic experiment, the hydrolysis of NPP in the presence of varying concentrations of molybdate was followed by ^1H NMR spectroscopy. The pH of the solution was measured in the beginning and at the end of the hydrolytic reaction, and the difference was typically less than 0.1 pH unit. The pD value of the solution was obtained by adding 0.41 to the pH reading, according to formula pD = pH + 0.41.[48] The reaction samples were kept at constant temperature and the rate constants for the hydrolysis were determined by following the appearance of the *p*-nitrophenol resonances in the ^1H NMR spectra at different time intervals. The observed first order rate constants (k_{obs}) were calculated by the integral method from at least 90% conversion. For reactions performed in H_2O solutions, the same kinetic method was used, and the reaction products were detected by the ^1H NMR water suppression technique.

RESULTS AND DISCUSSION

Hydrolysis of NPP by Polyoxomolybdate. Acidification of a molybdate solution leads to the formation of isopolyoxomolybdates so that at any given pH below 6.5 the presence of two or more species has been detected.[49] The first cluster that is formed in mildly acidic solutions is heptamolybdate $[Mo_7O_{24}]^{6-}$ and its protonated forms, while further acidification leads to the formation of octamolybdate $[Mo_8O_{26}]^{6-}$:

$$7[MoO_4]^{2-} + 8H^+ \rightleftharpoons [Mo_7O_{24}]^{6-} + 4H_2O$$

$$8[MoO_4]^{2-} + 12H^+ \rightleftharpoons [Mo_8O_{26}]^{4-} + 6H_2O$$

The initial reaction between a solution containing 700 mM $[MoO_4]^{2-}$ and 100 mM NPP was performed at pD 5.10. According to the thermodynamic model developed previously

Scheme 1. Hydrolytic Cleavage of NPP Promoted by $[Mo_7O_{24}]^{6-}$

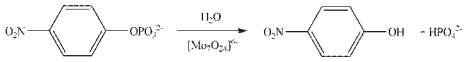

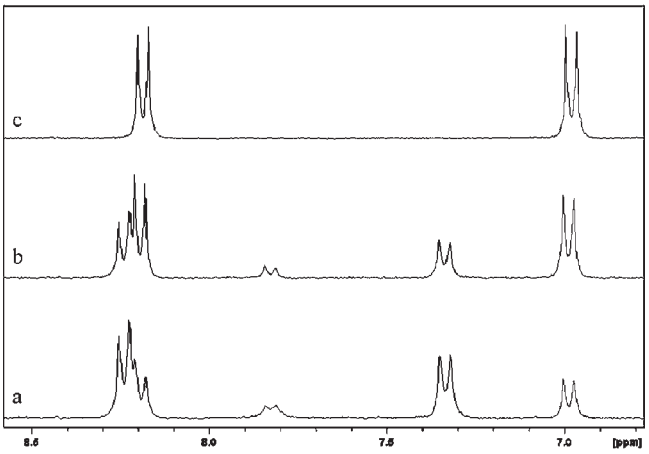

Figure 1. ^{1}H NMR spectra of the reaction between 700 mM $[MoO_4]^{2-}$ and 100 mM NPP at pD 5.10 and 50 °C after (a) 1 h, (b) 3 h, and (c) 24 h after mixing.

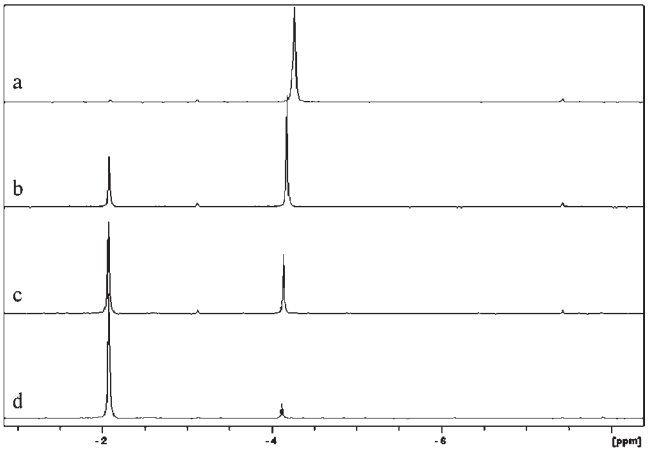

Figure 2. ^{31}P NMR spectra recorded during the reaction of 100 mM NPP with 700 mM $[MoO_4]^{2-}$ at pD 5.1 recorded (a) upon mixing, (b) after 2 h, (c) after 5 h, and (d) after 13 h.

in our group, at this pD value $[Mo_7O_{24}]^{6-}$ is the major species in solution.[45] During the course of the reaction, ^{1}H NMR spectra of the aromatic region indicated the disappearance of the NPP resonances at 8.25 and 7.33 ppm and the appearance of the *p*-nitrophenol (NP) resonances at 8.20 and 6.95 ppm (Figure 1). This is clear evidence that the cleavage of the labile phosphoester bond in NPP occurred. The NMR spectra did not show evidence of any paramagnetic species, excluding the possibility of Mo(VI) reduction to Mo(V), and indicating that the cleavage of the phosphodiester bond is purely hydrolytic. (Scheme 1).

A close inspection of the ^{1}H NMR spectra revealed the existence of another minor species in solution, characterized by a doublet at 7.83 ppm. Although present during the course of reaction, this species fully disappear upon completion of NPP hydrolysis.

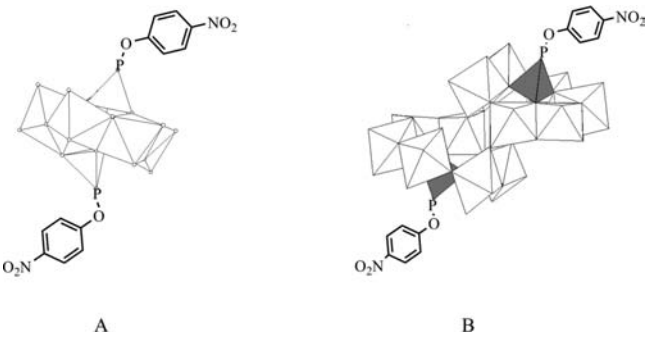

Figure 3. Structure of complex A, $(NPP)_2Mo_5O_{21}^{4-}$ and complex B, $(NPP)_2Mo_{12}O_{36}(H_2O)_6^{4-}$.

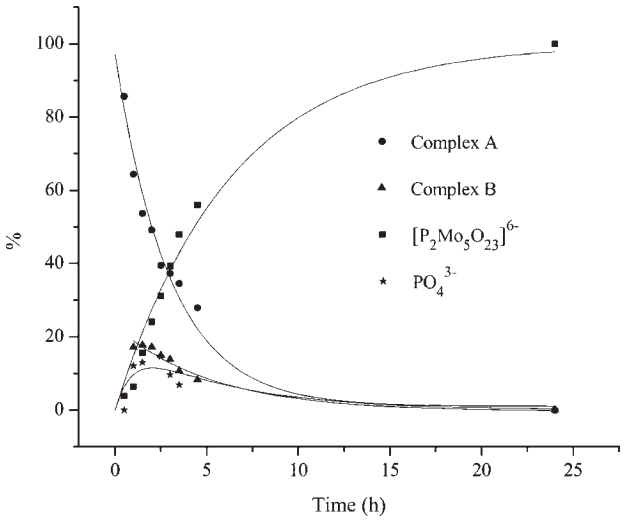

Figure 4. Fraction of NPP, complex A, complex B, phosphate, and $[P_2Mo_5O_{23}]^{6-}$ of a solution containing 100 mM NPP and 700 mM $[MoO_4]^{2-}$ at pD 5.2 followed by ^{31}P NMR.

The ^{31}P NMR spectra (Figure 2) recorded shortly upon mixing of NPP and $[Mo_7O_{24}]^{6-}$ have shown the absence of free NPP resonance at −5.95 ppm and appearance of two new resonances at −4.27 ppm and −7.42 ppm. This indicates that NPP was fully bound into two types of complexes designated **A** and **B**, which were present in about a 9:1 ratio.

DOSY NMR spectroscopy suggested that complex A has a formula $(NPP)_2Mo_5O_{21}^{4-}$, consisting of five MoO_6 octahedra coupled by one corner- and four edge-shared units to form a ring structure, which is capped on either side by two phosphate moieties, and is characterized by a ^{31}P NMR resonance at −4.27 ppm.[45] Complex B with the formula $(NPP)_2Mo_{12}O_{36}(H_2O)_6^{4-}$ is built up of two weakly binding $(NPP)Mo_6O_{18}(H_2O)_3$ entities and gives a ^{31}P NMR signal at −7.42 ppm (Figure 3).

During the course of the reaction a small peak at −3.12 ppm appeared and disappeared again. Spiking experiments identified this peak as free phosphate. At the end of the hydrolysis reaction a single peak at −2.05 ppm was detected. This peak could be unambiguously assigned to $[P_2Mo_5O_{23}]^{6-}$. The separately prepared pentamolybdodiphosphate ion $[P_2Mo_5O_{23}]^{6-}$, which typically forms in mildly acidic solutions containing molybdate and phosphate ions exhibited the same NMR features as the final complex observed at the end of hydrolytic reaction.[50]

dx.doi.org/10.1021/ic201498u |*Inorg. Chem.* 2011, 50, 11552–11560

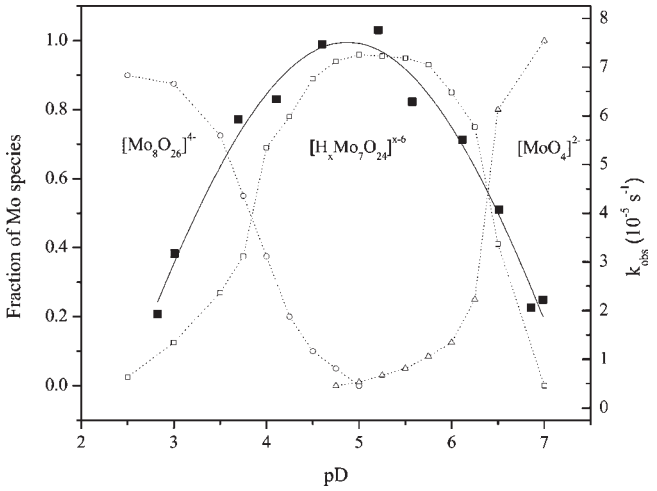

Figure 5. pD dependence of k_{obs} for the hydrolysis of 100 mM NPP in the presence of 700 mM $[MoO_4]^{2-}$ at 50 °C (solid line). Distribution of molybdate species as a function of pD was added for comparison (dotted line).

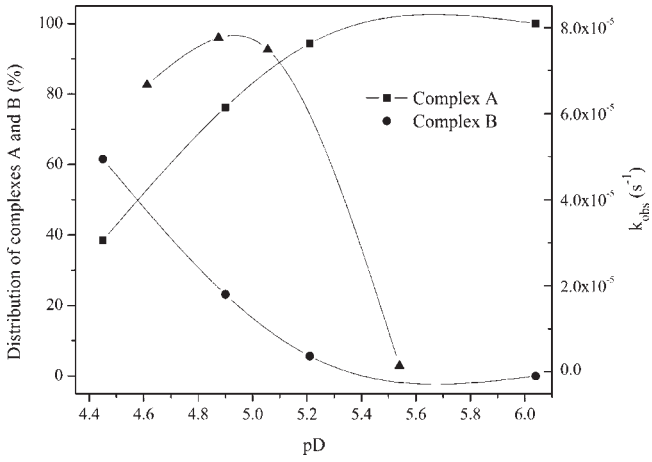

Figure 6. Distribution of complexes A and B as a function of pD. The pD dependence of k_{obs} (solid triangles) was added for comparison.

Figure 4 summarizes the species distribution which was obtained by integration of the ^{31}P NMR spectra, recorded at different time increments.

The first-order rate constants (k_{obs}) for the hydrolysis of NPP were calculated from the increase in intensity of the *p*-nitrophenol (NP) ^{1}H NMR resonances at different reaction times. A first-order exponential fit resulted in a rate constant of 2.73×10^{-5} s^{-1}. The same reaction was studied by following the increase of the NP absorption band maximum at 315 nm by UV−Vis spectroscopy and resulted in a comparable value for the rate constant (3.20×10^{-5} s^{-1}). It has to be noted that despite the presence of an activating nitrophenyl group, the phosphoester bond in NPP is still extremely stable. At 50 °C the half-life for P−O bond cleavage was estimated to be 135 days. In that respect, the molybdate accelerates the rate of phosphoester bond hydrolysis by nearly 3 orders of magnitude. Contrary to NPP hydrolysis, the hydrolysis of phenylphosphate (PP) was very slow. After 1 day at 50 °C only a small amount (2%) of a 100 mM solution of PP was hydrolyzed to the corresponding phenol and inorganic phosphate in the presence of 700 mM $[MoO_4]^{2-}$, while in the case of NPP almost 90% conversion was achieved under the same conditions. Further accurate analysis of the PP reaction was not possible because of the formation of a white precipitate.

pD Dependence of the Hydrolysis Rate. To identify the hydrolytically active molybdate complex, the effect of pD on the hydrolysis of NPP was studied. The fact that the reactivity follows the pD profile of a certain species suggests that k_{obs} is proportional to the concentration of that species. Since the kinetic measurements were performed in D_2O solutions, the rates were plotted as a function of pD, which was obtained by adding 0.41 pH units to the recorded pH value.[48] This is illustrated in Figure 5, where the values of k_{obs} and the fraction of polyoxometalate species are plotted as a function of pD.

The pD dependence of k_{obs} shows a bell-shaped profile with the fastest cleavage observed at pD 5.0. Comparison of the rate profile with the concentration profile of polyoxometalates shows a good overlap of k_{obs} and the concentration of $[Mo_7O_{24}]^{6-}$, implying that presence of heptamolybdate is required for the hydrolytic reaction to occur. Indeed, the highest rates were observed between pD 4.0 and 6.0 where $[Mo_7O_{24}]^{6-}$ predominates in solution. Although at the examined pD range other molybdenum(VI) species such as $[MoO_4]^{2-}$ and $[Mo_8O_{26}]^{4-}$ are present in solution, they seem to be catalytically much less active. Slow hydrolysis at lower pD values, where $[Mo_8O_{26}]^{4-}$ predominates, implies low catalytic activity of this species. Furthermore, hydrolysis hardly occurred at pD 8.0 where $[MoO_4]^{2-}$ is the only Mo(VI) species present in solution, suggesting that the monomeric form is virtually hydrolytically inactive.

Binding of NPP to Polyoxomolybdates. While the pD dependence of the rate constant implies that $[Mo_7O_{24}]^{6-}$ is the hydrolytically active species in solution, the ^{31}P NMR and DOSY measurements with the PhP analogue suggest that NPP is completely bound into complexes A and B upon mixing with $[Mo_7O_{24}]^{6-}$.[45,51,52] The pD dependent formation of complexes A and B (Figure 6) shows that the ratio between complexes A and B is strongly dependent on the pD. Upon decrease in pD of the solution, the amount of complex B gradually increased. While at pD 6.04 complex A is the only NPP containing structure, at pH 4.4 only about 40% of this complex is detected in solution. The ^{1}H and ^{31}P NMR experiments at pD 7.0 and 8.0 show no evidence of the formation of the complex A and B. This may explain the slow hydrolysis of NPP at these pD values and suggest that the formation of complexes A and B is essential for the hydrolysis to be observed. To correlate the distribution of complexes A and B to the reaction rate, the pD dependency of the reaction rate constant was added for comparison. No clear correlation can be observed, implying that both complexes A and B lead to hydrolysis of NPP. It is however possible that the NPP hydrolysis rate constant is different for both complexes and that k_{obs} therefore represents a cumulative value.

The hydrolysis of NPP in the presence of $[Mo_7O_{24}]^{6-}$ was also analyzed by ^{95}Mo NMR spectroscopy (Figure 7). A 700 mM solution of $[MoO_4]^{2-}$ at pH 5.1 is characterized by two peaks: a sharp peak at 0 ppm which corresponds to $[MoO_4]^{2-}$ and a broad resonance at 35 ppm that can be assigned to $[Mo_7O_{24}]^{6-}$.[53] Upon adding NPP a significant broadening of the 0 ppm resonance was observed. At the end of the hydrolytic reaction the intensity of the peak at 35 ppm was strongly diminished and the species at 0 ppm remained as a major component in solution. ^{95}Mo NMR control experiments of a 100 mM $[P_2Mo_5O_{23}]^{6-}$ solution confirmed that this species is

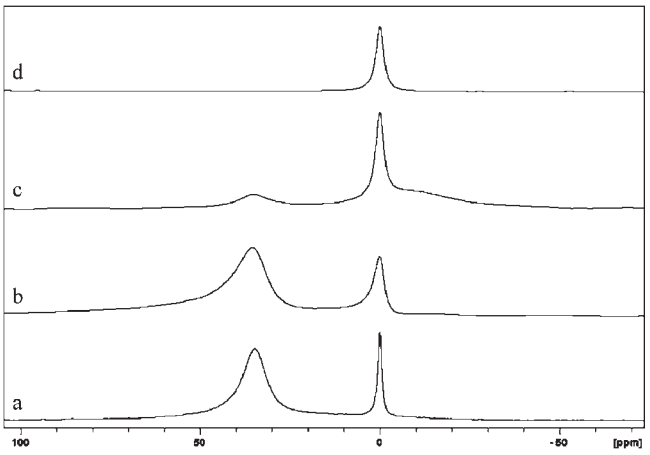

Figure 7. ^{95}Mo NMR spectra of (a) 700 mM solution of $[MoO_4]^{2-}$ at pD 5.1, (b) 700 mM solution of $[MoO_4]^{2-}$ upon adding 100 mM solution of NPP at pD 5.1, (c) mixture b at the end of hydrolytic reaction, and (d) 100 mM solution of $[P_2Mo_5O_{23}]^{6-}$ at pD 5.1.

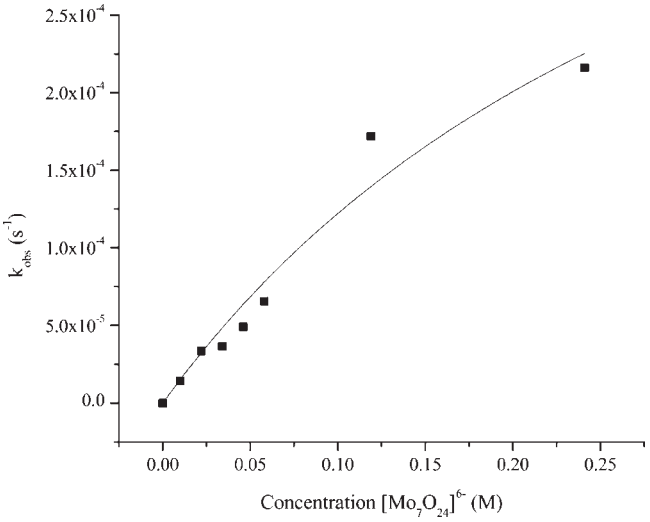

Figure 8. k_{obs} as a function of the concentration of $[Mo_7O_{24}]^{6-}$. The concentration of NPP was kept constant at 20 mM.

characterized by a broad resonance at 0 ppm. Considering the very similar environment of molybdenum atoms in $[P_2Mo_5O_{23}]^{6-}$ and the complex A, it is likely that the ^{95}Mo chemical shift in these two complexes is very similar. Bearing in mind the results from ^{31}P NMR measurements, which unambiguously prove complete binding of NPP to the polyoxomolybdate structure, the broadening of the peak at 0 ppm can be interpreted as the formation of complex A which is gradually converted into $[P_2Mo_5O_{23}]^{6-}$ in the course of NPP hydrolysis. The disappearance of the $[Mo_7O_{24}]^{6-}$ peak at 35 ppm occurs as a consequence of the equilibrium shift due to the binding of these species into complex A, which is being consumed during the hydrolytic reaction.

To estimate the equilibrium constant for the binding between NPP and $[Mo_7O_{24}]^{6-}$, kinetic experiments using a fixed amount of NPP and increasing amounts of $[MoO_4]^{2-}$ at pH 5.2 and 50 °C were examined by ^{1}H NMR spectroscopy (Figure 8). The overall reaction scheme can be written as presented in Scheme 2.

Scheme 2. Binding of NPP to $[Mo_7O_{24}]^{6-}$

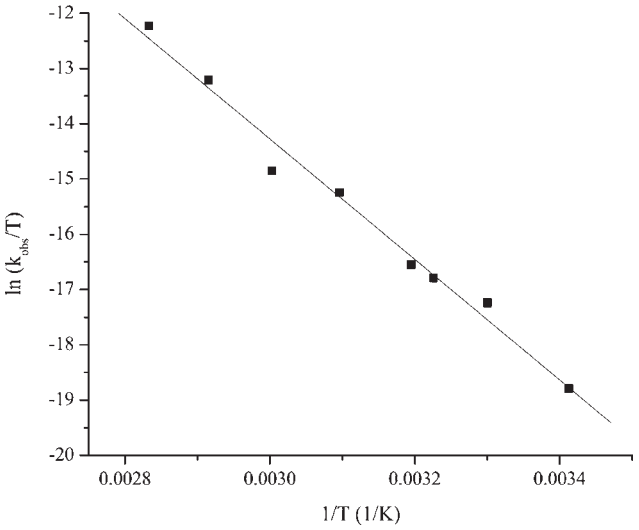

Figure 9. $\ln(k_{obs}/T)$ as a function of temperature for the hydrolysis of NPP.

Since ^{31}P NMR experiments indicated that the binding between NPP and $[Mo_7O_{24}]^{6-}$ is fast, it is reasonable to assume that the formation of the product (k_2) is much slower than reaching the equilibrium between NPP and molybdate, $k_1 + k_{-1} \gg k_2$. Because the formation of nitrophenol (NP) is a first-order reaction, k_{obs} can be written as in eq 1.

$$k_{obs} = \frac{k_2[Mo_7O_{24}^{6-}]_0}{\frac{k_{-1}}{k_1} + [Mo_7O_{24}^{6-}]_0} \quad (1)$$

The ratio between k_1 and k_{-1} is equal to the formation constant, K_f. By fitting eq 1 to the data in Figure 8, k_2 (5.60×10^{-4} s^{-1}) and K_f (361.2 M^{-1}) were calculated. It is important to note that since at this pH both complexes A and B were present in solution, the calculated binding constant represents an average value.

Temperature Dependence of the Hydrolytic Reaction. The effect of temperature on k_{obs} was determined in the temperature range between 293 and 353 K. As expected, an increase of temperature resulted in higher reaction rate constants. The activation Gibbs function ($\Delta G^{\ddagger}$ = 38 kJ mol^{-1} at 310 K), enthalpy ($\Delta H^{\ddagger}$ = 96 kJ mol^{-1}) and entropy ($\Delta S^{\ddagger}$ = −122 J mol^{-1} K^{-1}) were obtained from the Eyring plot (Figure 9). There is a close correspondence in the $\Delta H^{\ddagger}$ and $\Delta S^{\ddagger}$ values to the previously reported values for the hydrolysis of phopshoesters catalyzed by various metal complexes.[54−56] The negative activation entropy typically implies a largely ordered transition state and the increase of coordination number of phosphorus from four to five through formation of a trigonal-bipyramidal transition state. However, the activation parameters need to be interpreted with caution as they are usually derived from composite rate constants that also include the contribution from the binding of the ligand to the complex. Activation entropy is considered to be a mixture of factors

dx.doi.org/10.1021/ic201498u |Inorg. Chem. 2011, 50, 11552–11560

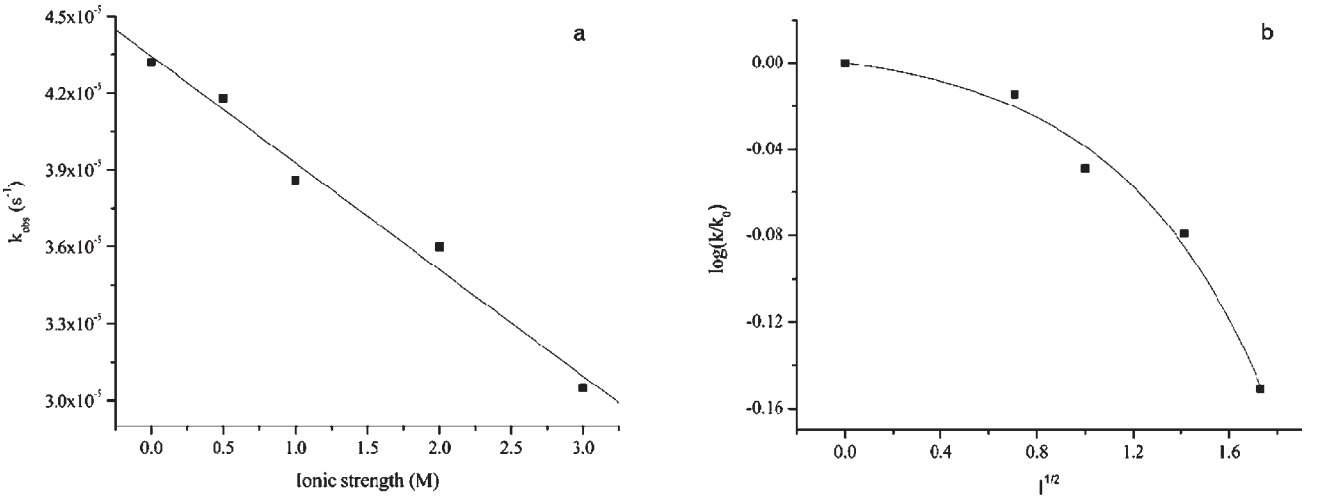

Figure 10. (a) Influence of the concentration of $NaClO_4$ on the rate constant for the reaction between 100 mM NPP with 700 mM $[MoO_4]^{2-}$. (b) $\log(k_{obs}/k_0)$ a function of the square root of the ionic strength.

(changes in solvation, conformation, molecularity, etc.) that are not easily predicted or rationalized. Therefore, assessing whether the change in activation entropy reflects a change in the reaction mechanism or in the binding of the phosphoester to the complex is not straightforward.

Effect of Ionic Strength of the Hydrolytic Rate. Ionic strength plays an important role in reactions between charged species. It highly affects the interaction between both reactants and has a pronounced influence on the reaction rate. The effect of salt ions on k_{obs} was investigated by adding increasing amounts of $NaClO_4$ or NaCl to a reaction mixture containing NPP and $[MoO_4]^{2-}$. As can be seen from Figure 10a, a reaction rate decrease was observed upon addition of increasing amounts of $NaClO_4$. The same effect was observed upon addition of NaCl. This can be related to the Olson−Simonson effect occurring for reactions between ions of the same sign, which predicts a rate decrease upon increasing the concentration of oppositely charged ions.[57] The effect of added salt on the rate constant for the reaction between two charged species A and B can be also described by the Brønsted−Bjerrum relationship (eq 2) in which $\log(k_{obs}/k_0)$ is plotted as a function of the square root of the ionic strength (Figure 10b).

$$\log \frac{k_{obs}}{k_0} = 1.018 Z_A Z_B I^{1/2} \qquad (2)$$

In this equation k_0 represents the reaction rate constant in the absence of salt, Z_A and Z_B the charge of both reactants, and I the ionic strength. Non-linearity of this plot implies that the salt concentration does not only influence the hydrolysis rate, but that it also exhibits a secondary effect, which is not surprising as it is well-known that ionic strength can also play a role in speciation and stability of the polyoxometalate species.[2−4,49]

EXAFS Spectroscopy. The molybdenum K-edge (located at 19999 eV) was used to investigate the coordination sphere of the molybdenum atoms during the hydrolysis of NPP. While ^{31}P NMR spectroscopy allows for the detection of the complexes A and B, as well as of the final complex $[P_2Mo_5O_{23}]^{6-}$, which all contain phosphorus atoms, it does not give an insight into the fate of other polyoxomolybdate species that do not contain phosphorus atoms. The EXAFS measurements were performed in a time period of approximately 24 h. During this period of time, a gradual decrease of the intensity of the Mo···Mo shell at 3.2 Å occurs, indicating a steady disappearance of the $[Mo_7O_{24}]^{6-}$ cluster. Apart from a reference solution containing only the $[Mo_7O_{24}]^{6-}$ species, in which no NPP was present, a total of eight samples have been measured. The first one (solution 1) was measured just after mixing NPP with $[Mo_7O_{24}]^{6-}$ at room temperature. Then, the mixture was heated to 50 °C and samples were taken from this solution at different time increments (solutions 2 until 8).

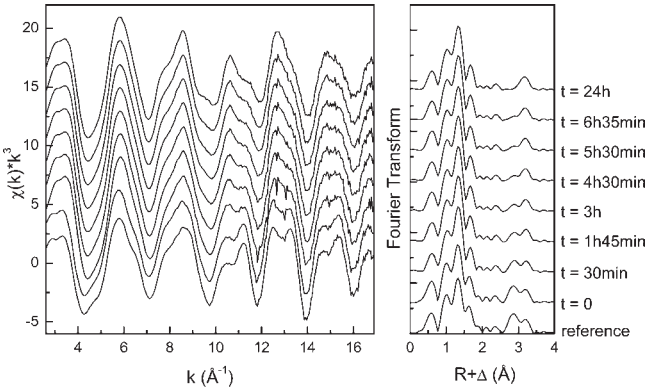

Figure 11. Raw k^3 weighted EXAFS (left) and corresponding Fourier transforms (right) of the 9 solutions.

The raw k^3 weighted Mo K-edge EXAFS spectra and the corresponding Fourier transforms of the 9 solutions are shown in Figure 11. The Fourier transforms show two distinctive sets of peaks: a first set, centered at about $R + \Delta = 1.3$ Å, corresponding to the overlapping Mo···O shells in the range of real distances 1.7−2.4 Å, and a second, centered at about $R + \Delta = 3$ Å, corresponding to the Mo···Mo shells at real distances of 3.2 and 3.4 Å, respectively.

In the left part of Figure 11, a gradual change in the raw k^3 weighted EXAFS spectra can be seen. The oscillations between $k = 10$ and $k = 16$ show the clearest changes. The Fourier transforms in the right part of Figure 11 show the clearest change at around $R + \Delta = 3$ Å, indicating that structural changes are occurring in the polyoxomolybdates present in the solution.

dx.doi.org/10.1021/ic201498u |*Inorg. Chem.* 2011, 50, 11552–11560

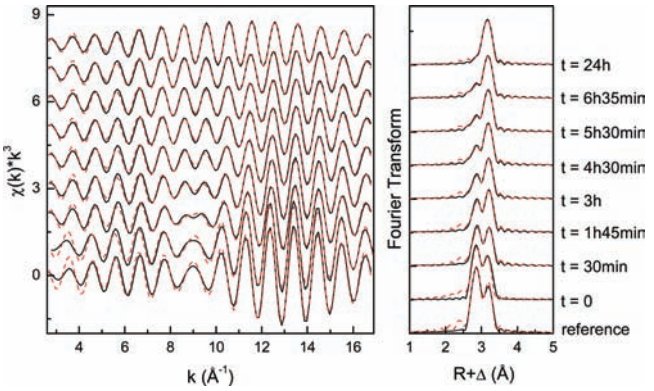

Figure 12. Back Fourier-transformed EXAFS signals (left) and Fourier transform windows (right) taken from Figure 11. Black solid lines are experimental curves; red dashed lines are fitted curves.

Table 1. EXAFS Structural Parameters for the Solution Containing 700 mM $[Mo_7O_{24}]^{6-}$ and 100 mM NPP at pD = 5.1

	N^a	R^a (Å)	σ^2 (Å^2)	$\Delta E_{k=0}$ (eV)	F
Reference	1.71[b]	3.23	0.00526	4.0	0.25
(no NPP)	1.71[b]	3.40	0.00603		
Solution 1	1.57	3.22	0.00526[b]	3.8	0.23
t = 0	1.64	3.40	0.00603[b]		
Solution 2	1.03	3.23	0.00526[b]	10.1	0.11
t = 30 min	1.23	3.40	0.00603[b]		
Solution 3	0.95	3.23	0.00526[b]	10.6	0.09
t = 1 h 45 min	1.34	3.40	0.00603[b]		
Solution 4	0.80	3.23	0.00526[b]	10.7	0.07
t = 3 h	1.27	3.40	0.00603[b]		
Solution 5	0.72	3.23	0.00526[b]	10.9	0.06
t = 4 h 30 min	1.28	3.40	0.00603[b]		
Solution 6	0.64	3.23	0.00526[b]	11.1	0.05
t = 5 h 30 min	1.26	3.40	0.00603[b]		
Solution 7	0.61	3.23	0.00526[b]	11.1	0.05
t = 6 h 35 min	1.26	3.40	0.00603[b]		
Solution 8	0.42	3.22	0.00526[b]	11.7	0.04
t = 24 h	1.23	3.40	0.00603[b]		

[a] Errors in coordination numbers N are ±10%; errors in distances R are ±0.01 Å. [b] Value fixed during shell-fit procedure. The overall goodness of the fits, F, is given by χ^2, weighted by the magnitude of data. The threshold energy, $E_{k=0}$, was arbitrarily defined at 19999 eV and varied as a global fit parameter resulting in the energy shift $\Delta E_{k=0}$.

Because the $[Mo_7O_{24}]^{6-}$ species is in constant equilibrium with the $[MoO_4]^{2-}$ monomer, it is not possible to obtain a reasonable fit including the Mo···O shells. The peaks at $R + \Delta$ = 3 Å, however, allow the identification of the polyoxomolybdate in solution. Indeed, close examination of the crystal structure of the $[Mo_7O_{24}]^{6-}$ cluster reveals that there are basically two sets of Mo···Mo distances in this molecule: one centered at 3.2 Å, and another one centered at 3.4 Å.[56] In the $[P_2Mo_5O_{23}]^{6-}$ cluster, however, which would result from the reaction between $[Mo_7O_{24}]^{6-}$ and phosphate, all Mo···Mo distances are more or less the same and centered at 3.4 Å. So, monitoring the amplitude of the Mo···Mo shell at 3.2 Å allows to follow the change in the concentration of $[Mo_7O_{24}]^{6-}$.

Therefore, a back-transformation from FT to $\chi(k)$ in the range of the Mo···Mo shells was made to give the corresponding EXAFS oscillations. These were then fitted with two Mo···Mo shells. This Fourier-filtered data range, taken from the spectra in Figure 11, is shown in Figure 12. The experimental curves are given as the black solid lines, and the fitted curves are given as the red dashed lines. Careful calculation from the crystal data indicates that every Mo atom in the $[Mo_7O_{24}]^{6-}$ cluster "sees" on average 1.71 Mo neighbors at 3.2 Å, and also 1.71 Mo neighbors at 3.4 Å. These coordination numbers N have been fixed in the shell fit procedure for the reference solution, whereas the distances R and Debye−Waller factors σ^2 were left free. The fitted distances of 3.23 and 3.40 Å, respectively, correspond well to the distances obtained from the crystal structure. This indicates that the only polyoxomolybdate present in the reference solution is $[Mo_7O_{24}]^{6-}$, as could be expected.

In a second step, the Debye−Waller factors that were obtained from the fit of the reference solution were taken and fixed during the shell fit procedure of solutions 1 (time 0) until 8 (time 24 h) to obtain the coordination numbers in the Mo···Mo shells. The EXAFS structural parameters for the 9 solutions are summarized in Table 1.

From the right part of Figure 12, it is clear that the amplitude of the Mo···Mo shell at a real distance of 3.2 Å decreases steadily from the reference solution to the solution at time 24 h, whereas the amplitude of the shell at a real distance of 3.4 Å stays more or less the same (from Table 1, it can be seen that in fact also this shell decreases somewhat in intensity). This indicates that the $[Mo_7O_{24}]^{6-}$ cluster is gradually converted into the $[P_2Mo_5O_{23}]^{6-}$ cluster.

From looking at Figure 12 and Table 1, comparing the signals and data from the reference solution with those of the solution at time 0, it is noteworthy to mention that right after mixing the NPP solution with the $[Mo_7O_{24}]^{6-}$ solution, a small fraction of the $[Mo_7O_{24}]^{6-}$ cluster seems to have immediately reacted, even though the kinetics of the hydrolytic reaction are quite slow at room temperature. This is in agreement with the suggested equilibrium that is established between the $[Mo_7O_{24}]^{6-}$ cluster and the intermediate species A and B detected in ^{31}P NMR.

Assuming that the reaction has reached an end point at t = 24 h, one can estimate the remaining fraction of $[Mo_7O_{24}]^{6-}$, by taking the ratio between the coordination number for the Mo···Mo shell at 3.2 Å, from solutions 8 and 1. This indicates that about 25% of the $[Mo_7O_{24}]^{6-}$ cluster remains in solution. Theoretically, if all $[Mo_7O_{24}]^{6-}$ would be converted to $[P_2Mo_5O_{23}]^{6-}$, the coordination number for the Mo···Mo shell at 3.4 Å should increase to a value of 2, since every Mo atom in the $[P_2Mo_5O_{23}]^{6-}$ cluster "sees" on average two other molybdenum atoms at about 3.4 Å. However, both the fact that only about 75% of the $[Mo_7O_{24}]^{6-}$ cluster is converted into the $[P_2Mo_5O_{23}]^{6-}$ cluster and the fact that both of these clusters are in equilibrium with the $[MoO_4]^{2-}$ monomer (in which the molybdenum atom does not "see" any other molybdenum atoms) account for the observed slight decrease in the coordination number of the Mo···Mo shell at 3.4 Å.

CONCLUSION

In conclusion, we report on a DNA model phosphoester bond cleavage promoted by a highly negatively charged polyoxometalate cluster. Binding of NPP to $[Mo_7O_{24}]^{6-}$ results in the formation of two complexes A and B in which the phosphoester

group is incorporated into the polyoxomolybdate skeleton. The sharing of oxygen atoms with Mo(VI) centra may lead to bond strain and cause polarization of the P−O ester bond and its activation toward external attack by water. The cleavage seems to occur by a mechanism which is different to that of other currently known hydrolytically active metal complexes. The pD dependence of k_{obs} shows a bell-shaped profile with the fastest cleavage observed at pD 5.0. At physiological pH, the dominant molybdenum species is the mononuclear $[MoO_4]^{2-}$ which is proven to be hydrolytically inactive. However, in the lower pH environment associated with hypoxic tumors the catalytically active species at pH 5 may play a role in the biological activity of POMs. We are currently examining the phosphoesterase activity of polyoxomolybdate toward oligonucleotides and other DNA substrates. These studies are important since they may shed more light on the molecular origin of the biological activity of polyoxomolybdates.

AUTHOR INFORMATION

Corresponding Author

*E-mail: Tatjana.Vogt@chem.kuleuven.be. Fax: +32 16/327992.

ACKNOWLEDGMENT

G.A. thanks FWO-Flanders (Belgium) for the doctoral fellowship. T.N.P.-V. thanks K. U. Leuven for the financial support (START 1/09/028). We thank the FWO-Vlaanderen and The Netherlands Organization for Scientific Research (NWO) for providing beam time at the Dutch−Belgian Beamline (DUBBLE, BM26A, ESRF). Sergei Nikitenko and Miguel Silveira (DUBBLE) are acknowledged for technical support during the EXAFS measurements.

REFERENCES

(1) Pope, M. T.; Müller, A. *Angew. Chem., Int. Ed. Engl.* **1991**, *30*, 34.
(2) Pope, M. T. Polyoxo anions: Synthesis and Structure. In *Comprehensive Coordination Chemistry II*;Wedd, A. G., Ed.; Elsevier Science: New York, 2004; Vol.4, pp 635−678.
(3) Hill, C. L. Polyoxometalates: Reactivity. In *Comprehensive Coordination Chemistry II*; Wedd, A. G., Ed.; Elsevier Science: New York, 2004; Vol.4, pp 679−759.
(4) Pope, M. T., Müller, A., Eds.; *Polyoxometalate Chemistry: From Topology via Self-Assembly to Applications*; Kluwer: Dordrecht, The Netherlands, 2001.
(5) Kozhevnikov, I. V. *Chem. Rev.* **1998**, *98*, 198.
(6) Hill, C. L.; Prossermccartha, C. M. *Coord. Chem. Rev.* **1995**, *143*, 407.
(7) Proust, A.; Thouvenot, R.; Gouzerh, P. *Chem. Commun.* **2008**, 1837.
(8) Mizuno, N.; Yamaguchi, K.; Kamata, K. *Coord. Chem. Rev.* **2005**, *249*, 1944.
(9) Neumann, R. *Prog. Inorg. Chem.* **1998**, *47*, 317.
(10) Rhule, J. T.; Hill, C. L.; Judd, D. A. *Chem. Rev.* **1998**, *98*, 327.
(11) Yamase, T. J. *Mater. Chem.* **2005**, *15*, 4773.
(12) Hasenknopf, B. *Front. Biosci.* **2005**, *10*, 275.
(13) Wang, X. H.; Li, F.; Liu, S. X.; Pope, M. T. *J. Inorg. Biochem.* **2005**, *99*, 452.
(14) Gerth, H. U. V.; Rompel, A.; Krebs, B.; Boos, J.; Lanvers-Kaminsky, C. *Anti-Cancer Drugs* **2005**, *16*, 101.
(15) Cindric, M.; Novak, T. K.; Kraljevic, S.; Kralj, M.; Kamenar, B. *Inorg. Chim. Acta* **2006**, *359*, 1673.
(16) Fujita, H.; Fujita, T.; Sakurai, T.; Seto, Y. *Chemotherapy* **1992**, *40*, 173.
(17) Yamase, T.; Fujita, H.; Fukushima, K. *Inorg. Chim. Acta* **1988**, *151*, 15.
(18) Ogata, A.; Mitsui, S.; Yanagie, H.; Kasano, H.; Hisa, T.; Yamase, T.; Eriguchi, M. *Biomedicine & Pharmacotherapy* **2005**, *59*, 240.
(19) Yanagie, H.; Ogata, A.; Mitsui, S.; Hisa, T.; Yamase, T.; Eriguchi, M. *Biomed. Pharmacother.* **2006**, *60*, 349.
(20) Ogata, A.; Yanagie, H.; Ishikawa, E.; Morishita, Y.; Mitsui, S.; Yamashita, A.; Hasumi, K.; Takamoto, S.; Yamase, T.; Eriguchi, M. *Br. J. Cancer* **2008**, *98*, 399.
(21) Kolesarova, A.; Capcarova, M.; Sirotkin, A. V.; Medvedova, M.; Kalafova, A.; Filipejova, T.; Kovacik, J. *J. Environ. Sci., Health, Part A* **2011**, *46*, 170.
(22) Katsoulis, D. E.; Lambriandou, A. N.; Pope, M. T. *Inorg. Chim. Acta* **1980**, *46*, L55.
(23) Geraldes, C. F. G. C.; Castro, M. C. C. A. *J. Inorg. Biochem.* **1986**, *28*, 319.
(24) Piperaki, P.; Katsaros, N.; Katakis, D. *Inorg. Chim. Acta* **1982**, *67*, 37.
(25) Hill, L. M. R.; George, G. N.; Duhm-Klair, A. K.; Young, C. G. *J. Inorg. Biochem.* **2002**, *88*, 274.
(26) Kwak, W.; Pope, M. T.; Scully, T. F. *J. Am. Chem. Soc.* **1975**, *97*, 5735.
(27) Cartuyvels, E.; Van Hecke, K.; Van Meervelt, L.; Görller-Walrand, C.; Parac-Vogt, T. N. *J. Inorg. Biochem.* **2008**, *102*, 1589.
(28) Weil-Malherbe, H.; Green, R. H. *Biochem. J.* **1951**, *49*, 286.
(29) Ishikawa, E.; Yamase, T. *J. Inorg. Biochem.* **2006**, *100*, 344.
(30) Cleland, W. W.; Hengge, A. C. *Chem. Rev.* **2006**, *106*, 3255.
(31) Williams, N. H.; Takasaki, B.; Wall, M.; Chin, J. *Acc. Chem. Res.* **1999**, *32*, 485.
(32) Morrow, J. R.; Iranzo, O. *Curr. Opin. Chem. Biol.* **2004**, *8*, 192.
(33) Mancin, F.; Scrimin, P.; Tecilla, P.; Tonellato, U. *Chem. Commun.* **2005**, 2540.
(34) Ott, R.; Krämer, R. *Angew. Chem., Int. Ed.* **2000**, *39*, 3255.
(35) Fanning, A. M.; Plush, S. E.; Gunnlaugsson, T. *Chem. Commun.* **2006**, 3791.
(36) Aguilar-Perez, F.; Gomez-Tagle, P.; Collado-Fregoso, E.; Yatsimirsky, A. K. *Inorg. Chem.* **2006**, *45*, 9502.
(37) Feng, G.; Natale, D.; Prabaharan, R.; Mareque-Rivas, J. C.; Williams, N. H. *Angew. Chem., Int. Ed.* **2006**, *45*, 7056.
(38) Schneider, H.-J.; Rammo, J.; Hettich, R. *Angew. Chem., Int. Ed. Engl.* **1993**, *32*, 1716.
(39) O'Donoghue, A.; Pyun, S. Y.; Yang, M. Y.; Morrow, J. R.; Richard, J. P. *J. Am. Chem. Soc.* **2006**, *128*, 1615.
(40) Komiyama, M.; Kina, S.; Matsumura, K.; Sumaoka, J.; Tobey, S.; Lynch, V. M.; Anslyn, E. *J. Am. Chem. Soc.* **2002**, *24*, 13731.
(41) Mitić, N.; Smith, S. J.; Neves, A.; Guddat, L. W.; Gahan, L. R.; Schenk, G. *Chem. Rev.* **2006**, *106*, 3338.
(42) Neves, A.; Lanznaster, M.; Bortoluzzi, A. J.; Peralta, R. A.; Casellato, A.; Castellano, E. E.; Herrald, P.; Riley, M. J.; Schenk, G. *J. Am. Chem. Soc.* **2007**, *129*, 7486.
(43) Cartuyvels, E.; Absillis, G.; Parac-Vogt, T. N. *Chem. Commun.* **2008**, 85.
(44) Absillis, G.; Cartuyvels, E.; Van Deun, R.; Parac-Vogt, T. N. *J. Am. Chem. Soc.* **2008**, *130*, 17400.
(45) Van Lokeren, L.; Cartuyvels, E.; Absillis, G.; Willem, R.; Parac-Vogt, T. N. *Chem. Commun.* **2008**, 2774.
(46) (a) Borsboom, M.; Bras, W.; Cerjak, I.; Detollenaere, D.; van Loon, D. G.; Goedtkindt, P.; Konijnenburg, M.; Lassing, P.; Levine, Y. K.; Munneke, B.; Oversluizen, M.; van Tol, R.; Vlieg, E. *J. Synchrotron Radiat.* **1998**, *5*, 518. (b) George, N. G.; Pickering, I. J. *EXAFSPAK, a suite of computer programs for analysis of X-ray absorption spectra*; Stanford Synchrotron Radiation Laboratory: Stanford, CA, 2000.
(47) Ankudinov, A. L.; Ravel, B.; Rehr, J. J.; Conradson, S. D. *Phys. Rev. B* **1998**, *58*, 7565.
(48) Glasoe, P. K.; Long, F. A. *J. Phys. Chem.* **1960**, *64*, 188.
(49) Cruywagen, J. J. *Adv. Inorg. Chem.* **2000**, *49*, 127.
(50) Pettersson, L.; Andersson, I.; Öhman, L.-O. *Inorg. Chem.* **1986**, *25*, 4726.

(51) Yagasaki, A.; Andersson, I.; Pettersson, L. *Inorg. Chem.* **1987**, *26*, 3926.
(52) Lyxell, D.-G.; Pettersson, L.; Persson, I. *Inorg. Chem.* **2001**, *40*, 584.
(53) Maksimovskaya, R. I.; Maksimov, G. M. *Inorg. Chem.* **2007**, *46*, 3688.
(54) Deal, K. A.; Hengge, A. C.; Burstyn, J. N. *J. Am. Chem. Soc.* **1996**, *118*, 1713.
(55) Deck, K. M.; Tseng, T. A.; Burstyn, J. N. *Inorg. Chem.* **2002**, *41*, 669.
(56) Fry, F H.; Fishermann, J.; Belousoff, M. J.; Spiccia, L.; Brügger, J. *Inorg. Chem.* **2005**, *44*, 941.
(57) Olson, A. R.; Simonson, T. R. *J. Chem. Phys.* **1946**, *17*, 1167.
(58) Sjobom, K.; Hedman, B. *Acta Chem. Scand.* **1973**, *27*, 3673.